

Profile driven interfaces in 1 + 1 dimensions : periodic steady states, dynamical melting and detachment

Abhishek Chaudhuri and Surajit Sengupta

*Satyendra Nath Bose National Centre for Basic Sciences, Block-JD, Sector-III,
Salt Lake, Calcutta - 700098.*

Abstract

We study the steady state structure and dynamics of a 2-d Ising interface placed in an inhomogeneous external field with a sigmoidal profile which moves with velocity v_e . In the strong coupling limit the problem maps onto an asymmetric exclusion process involving motion of particles in 1-d with position dependent right and left jump probabilities. For small v_e , the interface is stuck to the field profile. As v_e increases the profile detaches from the interface. At the transition point(and beyond), the interfacial structure and dynamics is characterized by KPZ exponents. For small v_e , on the other hand, the interface is macroscopically smooth with a vanishing roughness exponent α . The interfacial structure is periodic with a periodicity which depends on the orientation of the interface. For a fixed orientation this periodic structure “melts” as v_e is increased. We determine the dynamical “phase - diagram” of this system in the v_e - orientation plane.

Key words: Interface Dynamics, Kinetic Ising model, Dynamical phase transition
PACS: 05.10Gg,64.60.Ht,68.35.Rh

1 Introduction

Consider a one-dimensional (1-d) Ising interface [1,2] between up and down spins in two dimensions (2-d) obeying single-spin flip Glauber dynamics [3,4]. In the presence of a uniform driving field [5–10] the interface moves with a velocity which depends on the magnitude (and sign) of the driving field. On the other hand, a fixed external field profile which is positive in the region of up spins and negative in the region of down spins, would stabilize a stationary, macroscopically flat interface. In this paper we study systematically the structure and dynamics of this Ising interface as this field profile is moved

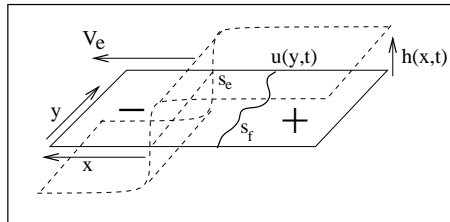


Fig. 1. An Ising interface $u(y,t)$ (bold curved line) between regions of positive (marked +) and negative (marked -) magnetization in an external, inhomogeneous field with a profile which is as shown (dashed line). The positions of the edge of the field profile and that of the front are labelled S_e and S_f respectively.

with an arbitrary velocity v_e .

There are two reasons why we are interested in this problem : Firstly, there are several important practical examples where inhomogeneous fields drive interfaces. Some of them include zone purification of Si where the controlled motion of a temperature field profile is used to preferentially segregate impurities[11], magnetization of a bar of iron with a permanent magnet, phase transitions induced by a travelling heat (welding) or pressure (metamorphosis of rocks) fronts etc. Secondly, we would like to extend this study, in the future, to the dynamics of solid interfaces where interfacial degrees of freedom are coupled to hydrodynamic modes of the bulk solid eg. phonons (acoustic emissions[11]) and defects[12]. A systematic study of how these modes are excited in sequence as v_e is increased is of great fundamental interest.

The object of our study here is the interface between up and down spin phases (Fig. 1) in the limit $h/J, T/J \rightarrow 0$, where J is the Ising exchange coupling, T the temperature and the field $h(x,t)$ here is inhomogeneous, $h = h_{max}$ in the region where the magnetization is positive and $-h_{max}$ in region where it is negative separated by a relatively sharp *edge*. The *edge* of the field (i.e. where the field changes sign) lies at S_e . The *front* or interface, $u(y,t)$ (no overhangs!) separates up and down spin phases. The interface is a bold curved line with the average position S_f . To move the interface we move the edge with velocity v_e ; in response the front moves with velocity v_f . Parts of the front which leads (lags) the edge of the field experience a backward (forward) force pulling it towards the edge. The driving force therefore varies in both space and time and depends on the relative position of the front compared to that of the edge of the dragging field. What is the behaviour of the front velocity v_f as a function of v_e ? What is the structure of the interface in various regimes? These are the questions we address in this paper.

Briefly, our results are as follows

- (1) For any orientation of the interface, $v_f = v_e$ for small v_e the front moves along with the field profile. We call this the “stuck” phase.
- (2) At a velocity $v_e = v_e^*$, the front detaches from the field profile. At higher values of v_e the front experiences an *uniform* magnetic field $h = h_{max}$

and the problem reduces to the growth of an Ising interface driven by a uniform field [5–10]

- (3) The structure of the “stuck” interface is flat with a roughness exponent $\alpha = 0$. Depending on the orientation of the interface, the height of the interface $u(y, t)$, as a function of y and time t , may show periodic oscillations in y and/or t . The nature of these oscillations depends crucially on the system size in a manner to be explained below.

In the next section we introduce a continuum description of the problem and derive the relevant coarse grained equations of motion. In Section 3 we present the mean field solution to these equations. In Section 4 we introduce fluctuations through an exact mapping to an asymmetric exclusion (particle hopping) model in 1-d and present, analyze and discuss our results obtained from computer simulations of this model. In Section 5 we present our conclusions.

2 Continuum Description

Let the magnetization of the 2-d Ising system be given by, $\phi \equiv \phi(x, y, t)$. We assume that for $h/J, T/J \rightarrow 0$ the magnetization is uniform everywhere except near the interface which may be parametrized by a function $u(y, t)$, where u is the height of the interface perpendicular to y . Hence the magnetization $\phi = \phi(x - u(y, t))$. The field profile is given by $h = h_{max} \tanh((x - v_e t)/\chi)$ where χ is the width of the profile. Model A dynamics[13] for ϕ then implies,

$$\frac{\partial \phi}{\partial t} = -\Gamma \frac{\delta H_T}{\delta \phi} + \zeta(\mathbf{r}, t) \quad (1)$$

where

$$H_T = \int d\mathbf{r} [a_1 \phi^2 + a_2 \phi^4 + a_3 (\nabla \phi)^2 - h(x, t) \phi] \quad (2)$$

is the Hamiltonian and ζ is a Gaussian white noise with zero mean and

$$\langle \zeta(\mathbf{r}, t) \zeta(\mathbf{r}', t') \rangle = 2k_B T \Gamma \delta(\mathbf{r} - \mathbf{r}') \delta(t - t') \quad (3)$$

Using H_T in Eq.1, taking $x - u(y, t) = v$ and converting all derivatives to derivatives over the profile $u(y, t)$, we have,

$$\begin{aligned}
-\phi'(v)\frac{\partial u}{\partial t} &= -\Gamma[2a_1\phi(v) + 4a_2\phi^3(v) - 2a_3\phi''(v) + 2a_3\phi'(v)\frac{\partial^2 u}{\partial y^2} \\
&\quad - 2a_3\phi''(v)(\frac{\partial u}{\partial t})^2 - h(x,t)] + \zeta(\mathbf{r},t)
\end{aligned} \tag{4}$$

We then choose a ϕ dependent mobility Γ contributing to the lowest order in ϕ consistent with symmetry viz. $\Gamma = \Gamma_0 + \Gamma_1(\nabla\phi)^2$. Substituting for Γ and integrating both sides of the equation with respect to x between limits $(u - \chi/2)$ and $(u + \chi/2)$ i.e. over the interfacial region, remembering that ϕ has a sigmoidal profile, we finally get an equation of motion for the profile u .

$$\frac{\partial u}{\partial t} = \lambda_1 \frac{\partial^2 u}{\partial y^2} - \lambda_2 \left(\frac{\partial u}{\partial y}\right)^2 \tanh\left(\frac{u - v_e t}{\chi}\right) - \lambda_3 \tanh\left(\frac{u - v_e t}{\chi}\right) + \zeta'(u, t) \tag{5}$$

where λ_1, λ_2 and λ_3 are constants. This is different from the familiar KPZ equation [10] in the fact that it lacks Galilean invariance ($u' \rightarrow u + \epsilon y$, $y' \rightarrow y - \lambda_2 \epsilon t$, $t' \rightarrow t$)

In general crystal field effects introduce a lattice periodic force [1] which may be accounted for by including an additional term $V_0 \sin(2\pi u/a)$ (a is the lattice parameter) to the right side of the above equation of motion.

3 Mean Field Result

A mean field calculation amounts to taking $u \equiv u(t)$ i.e. neglecting spatial fluctuations of the interface. Then

$$\frac{\partial u}{\partial t} = -\lambda_3 \tanh\left(\frac{u - v_e t}{\chi}\right) + \zeta'(u, t) \tag{6}$$

For large times ($t \rightarrow \infty$), $u \rightarrow v_f t$, where v_f is the average velocity of the front. Thus v_f is obtained by solving the self-consistency equation,

$$v_f = -\lambda_3 \tanh\left(\frac{(v_f - v_e)t}{\chi}\right) \tag{7}$$

In the $t \rightarrow \infty$ limit the hyperbolic tangent is replaced by the simply the sign of $v_f - v_e$ and is equivalent to taking $\chi \rightarrow 0$ namely, an infinitely sharp field profile. For small v_e the only solution to the self-consistency equation is $v_f = v_e$

as can easily be verified graphically. For large edge velocities $v_e > v_e^*$, where $v_e^* = \lambda_3$ we get $v_f = \lambda_3 = v_e^*$. We thus have a sharp transition from a region where the front follows the edge with the same velocity to one where it moves with a constant velocity unable to follow it anymore. The interface velocity relaxes to its steady state value v_e as $1/t$ in the region of low v_e . The region where the front moves with a constant velocity is evidently the well studied problem of driving an interface by a homogeneous field [6,9].

How is this result altered by including spatial fluctuations of u ? In order to answer this question we have mapped this interface model to an asymmetric exclusion process [14] and study the dynamics both analytically and numerically using computer simulations.

4 Beyond Mean Field Theory

The mapping to the exclusion process follows [8] by considering N_p particles distributed among N_s sites of a 1-d lattice. The particles are labelled $n = 1, 2, \dots, N_p$ sequentially at $t = 0$. Any configuration of the system is specified by the set of integers $\{y(n)\}$ where $y(n)$ denotes the location of the n th particle. In the interface picture n needs to be interpreted as a horizontal coordinate (y in Fig. 1), and $y(n)$ as a local height $u(y, t)$. Each configuration $\{y(n)\}$ then defines a one-dimensional interface inclined to the horizontal with mean slope $1/\rho$ where $\rho = N_p/N_s$. The interface coordinates satisfy $y(n+1) \geq y(n) + 1$, and periodic boundary conditions amount to setting $y(n+N_p) = y(n) \pm N_s$. Motion of the interface under the influence of a driving field corresponds to the hopping of particles. In each time step (N_p attempted hops), $y(n)$ tends to increase (or decrease) by 1 with probability p (or q); it actually increases (or decreases) if and only if $y(n+1) - y(n) > 1$. In our case the right and left jump probabilities p and q ($p + q = 1$) are not constants but themselves depend on the relative position of the interface $y(n)$ and the edge of the field $n/\rho + v_e t$. Note that in calculating this relative position we have to use the actual position of the interface *without* periodic boundary conditions. In our calculations reported here we use a bias $\Delta = p - q = \Delta_0 \text{sign}(y(n) - n/\rho - v_e t)$ with $\Delta_0 = 1$ unless otherwise stated. We are interested in the average vertical velocity of the interface v_f defined as the total number of particles moving right per time step. In addition to the front velocity, we also examine the behaviour of the width of the interface:

$$\sigma^2(t) = N_p^{-1} \sum_{n=1, N_p} \langle (y(n, t) - y(n, 0) - v_f t)^2 \rangle \quad (8)$$

as a function of time and system size N_s . The angular brackets denotes an average over the realizations of the random noise.

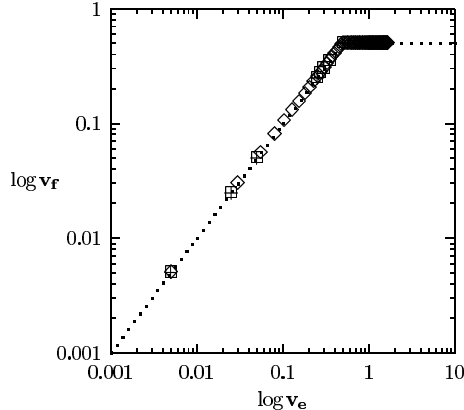


Fig. 2. The front velocity v_f as a function of the velocity of the dragging edge v_e for $N_s = 100(\square)$, $1000(\diamond)$, $10000(+)$ and $\rho = 0.5$. All the data (symbols, \square , \diamond , $+$) collapse on the mean field solution (dashed line).

Note that the usual particle hole symmetry for an exclusion process [5] is violated since exchanging particle and holes changes the relative position of the interface compared to the edge of the field.

4.1 Monte Carlo simulations for the dynamical transition

We perform Monte Carlo simulations of the exclusion process using a random sequential update [15] to understand the behavior of the interface in the presence of the inhomogeneous field profile. We study the system for different system sizes and densities and obtain the average velocity v_f of the steady state interface as a function of the velocity of the edge of the field profile v_e . The velocity v_f is obtained by dividing the distance moved by the interface for a certain (large) number of time steps by the total number of time steps after discarding the first few thousand steps to remove transients. Fig. 2 shows a sharp dynamical transition from an initially “stuck” interface with $v_f = v_e$ to a free, detached interface with $v_f = v_e^* = \Delta_0(1 - \rho)$ the result for an asymmetric exclusion process with density ρ . Note that the mean field solution for the front velocity and the dynamical transition is exact.

4.2 The Stuck phase ($v_e < v_\infty$)

The stuck phase is characterized by $v_f = v_e$ and σ bounded. To obtain the ground state of the interface in the presence of a stationary ($v_e = 0$) field profile it is sufficient to minimize $\sum_n (y(n) - n/\rho)^2$ which demands $y(n)$ to follow the edge n/ρ as closely as possible subject to the constraint that $y(n)$ be an integer. This ground state structure is always periodic for $\rho < 1/2$. For $\rho \geq 1/2$ this periodicity is destroyed for infinitesimal v_e . For densities which

are of the form $1/k$ where k is an integer, the result is particularly simple viz. $y(n) = kn$. This corresponds to a particle-hole system where the particles form a 1-d lattice with a lattice parameter of k . For an arbitrary density (orientation) the ground state is still periodic over short distances but has long-period (possibly incommensurate) modulations. We verify this by calculating the pair distribution function $g(l) = (1/N_p(N_p - 1)) \sum_{n,m} \delta_{l,(y(m)-y(n))}$, where n, m are particle indices and $m > n$. The Fourier transform of $g(l)$ shows prominent delta function peaks.

The dynamics of the interface for $v_e > 0$ depends on whether or not the system size is compatible with the lattice parameter k . If the system size N_s is an exact multiple of k then the particles which are separated by intervening regions of holes can move independently of each other in response to the local bias Δ . Let P_i be the probability ($\sum_{i=-\infty}^{\infty} P_i = 1$) of obtaining a particle (any particle) in state i where $i = 0$ corresponds to a particle which has not moved from its initial position and $i = s$ ($= -s$) corresponds to one which has moved s integral lattice spacings to the right (left) of its original position. Fluctuations of the interface about the ground state correspond to these independent particle motions which cost energy if $v_e t$ is integral. Consider now that $i < v_e t < i + 1$ the form of the bias Δ implies that the probabilities P_i satisfy the following set of master equations,

$$\begin{aligned} \dot{P}_j &= -P_j + P_{j+1} & \text{for } j > i + 1 \\ \dot{P}_j &= P_{j-1} - P_j + P_{j+1} & \text{for } j = i, i + 1 \\ \dot{P}_j &= -P_j + P_{j-1} & \text{for } j < i. \end{aligned} \tag{9}$$

Noting that the average position $S(t) = \langle N_p^{-1} \sum_n (y(n, t) - y(n, 0)) \rangle$ of the interface is given simply by $S(t) = \sum_{i=-\infty}^{\infty} i P_i(t)$ and $\sigma^2(t) = \sum_{i=-\infty}^{\infty} (i^2 - i) P_i(t)$ we obtain the results shown in Fig. 3(a) and 3(b). It is clear that these results match the corresponding ones obtained from Monte Carlo simulations exactly. The interface therefore follows the profile in a jerky fashion and the width of this interface oscillates between fixed bounds. Thus although the structure of the moving interface corresponds more or less with the ground state periodic structure for small v_e , the velocity is oscillatory. If however ρ is not the reciprocal of an integer and the system size does not accommodate an integral number of spatial periods of the ground state then the corresponding 1-d lattice contains long wavelength modulations and the particle hoppings are not independent anymore. For fixed edge velocities it is found that σ^2 is a constant in time independent of the size of the system, the constant, however, depends on v_e and ρ . The average position of the interface does not show any oscillations and faithfully follows the field profile corresponding exactly to the mean-field solution.

The Melting Transition

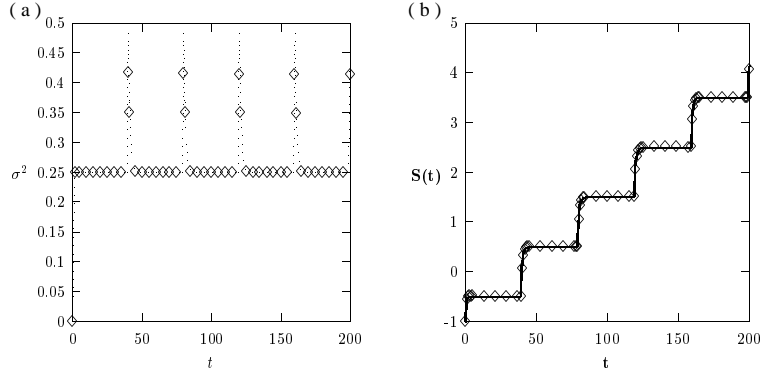


Fig. 3. (a) Variation of σ^2 with t for $\rho = 0.5$, $v_e = 0.025$ and $p = 1.0$ and (b) variation of $S(t)$ with t for $\rho = 0.5$, $v_e = 0.025$ and $p = 1.0$. Lines denote analytical results while points denote monte carlo data.

The Fourier transform of $g(n)$, i.e. the structure factor $\tilde{g}(q)$, indicates a “melting transition” of the periodic steady states with increasing v_e for any density ($\rho < 1/2$). We track this by plotting the intensity of the largest peak (smallest q) of $\tilde{g}(q_{max})$ as a function of v_e for a number of densities. This is shown in Fig.4(a). Also, the lattice parameter (a) obtained from $2\pi/q_{max}$ is used to determine the Lindemann ratio $L = \sigma^2/a^2$. The increase of the Lindemann ratio with the v_e for different densities (Fig. 4(b)) is another proof of a melting transition. These results are summarized in the dynamical phase diagram (Fig. 5) for the Ising interface in a moving field profile. It shows an detachment transition along the line $v_e = (1 - \rho)$ (for $\Delta_0 = 1$) and a melting transition. The exact position of this dynamical melting transition (unlike a thermodynamic transition) depends on the parameter used to characterize it. If we use $\tilde{g}(q_{max})$ then the melting transition occurs simultaneously with detachment for $\rho < 0.5$ and at $v_e = 0^+$ for larger ρ . Using the Lindemann parameter, however, one obtains a melting transition which preempts detachment.

5 Behavior at the transition point

We want to determine scaling form for $\sigma(t)$ at the transition point viz. the growth exponent β , the roughness exponent α and the dynamic exponent z . In the detached phase we know from renormalization group analysis that the exponents are in the Kardar-Parisi-Zhang (KPZ) universality class [1,10] viz. $\beta = 1/3$, $\alpha = 1/2$ and $z = \alpha/\beta = 3/2$. To determine these exponents at the transition point we make use of *Family-Vicsek scaling relation* [1]

$$\sigma(L, t) \sim N_s^\alpha f(t/N_s^z) \quad (10)$$

Fig. 6 shows the variation of t/N_s^z with $\sigma(L, t)/N_s^\alpha$ for different p and different

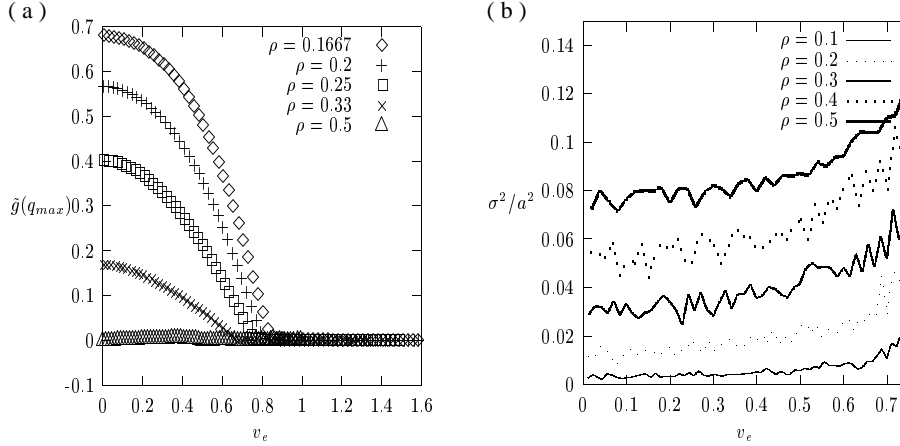


Fig. 4. (a) The structure factor $\tilde{g}(q_{max})$ vs. v_e for various ρ . Note that $\tilde{g}(q_{max})$ vanishes as v_e increases thereby implying a melting transition in the 1-d asymmetric exclusion process. (b) Variation of lindemann ratio L with edge velocity v_e for various densities. An increase of L again signifies melting.

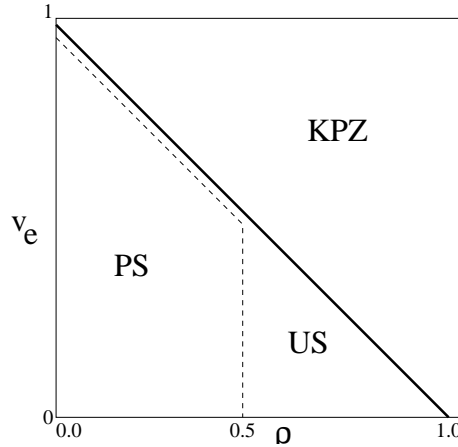


Fig. 5. Phase diagram for Ising interface driven by an inhomogeneous magnetic field showing periodic stuck (PS) steady states for $v_e < (1 - \rho)$ and $\rho < .5$, uniform stuck (US) steady states for $v_e < (1 - \rho)$ and $\rho > .5$ and detached (KPZ) steady states for $v_e \geq (1 - \rho)$.

system sizes N_s . The curves collapse onto one curve once an intrinsic width σ_i , arising from finite-size and crossover effects [1], is subtracted out. The exponents were found to be KPZ.

To understand why this happens we go back to our modified KPZ equation (Eq.5) and make the transformation $u = u' + v_f t$. We get

$$\begin{aligned} \frac{\partial u'}{\partial t} + v_f = \lambda_1 \frac{\partial^2 u'}{\partial y^2} - \lambda_2 \left(\frac{\partial u'}{\partial y} \right)^2 \tanh \left(\frac{(v_f - v_e)t + u'}{\chi} \right) \\ - \lambda_3 \tanh \left(\frac{(v_f - v_e)t + u'}{\chi} \right) + \zeta'(u, t) \end{aligned} \quad (11)$$

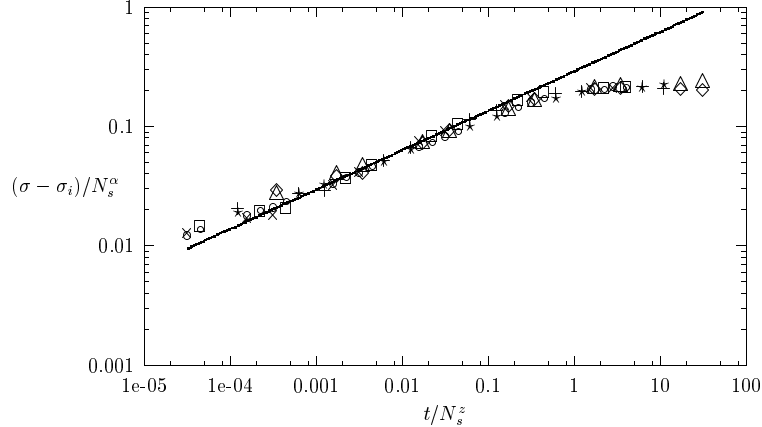


Fig. 6. Monte Carlo data $(\sigma - \sigma_i)/N_s^\alpha$ vs t/N_s^z for $p = 1.0$, $p = 0.7$ and with $N_s = 1000$ [\times, \circ], 800 [\square, \circ], 400 [$+, \star$], 200 [\diamond, \triangle]. All the curves collapse to a single universal function showing KPZ scaling.

Now substituting the mean field result for v_f (Eq.7), making use of the fact that at the transition point $v_f = \lambda_3$ and simplifying one can show that the above equation reduces to the familiar KPZ equation in u' .

6 Conclusion

In this paper we have studied the static and dynamical properties of an Ising interface in 2-d subject to a non-uniform, time-dependent external magnetic field. The system has a rich dynamical phase diagram with several dynamical phases (steady states). The nature of these steady states depend on the orientation of the interface and the velocity of the external field profile. The detailed dynamics of the interface depends on whether or not the size of the system is commensurate with the orientation. For a commensurate system, the interface follows the field in a jerky fashion and the width of the interface fluctuates between well defined bounds. For a general, incommensurate interface the motion of the interface is steady and the width is constant. For large velocities of the external field, the interface detaches from the profile and coarsens over time with KPZ exponents

In future we would like to study in detail further dynamical aspects of this system e.g. the hysteretic response of this system under time varying external parameters (v_e).

Acknowledgement: The authors would like to thank M. Barma, J. Krug, J.K. Bhattacharya, P. A. Sreeram and S. Majumdar for useful discussions. One of the authors (A.C.) thanks the Council of Scientific and Industrial Research (C.S.I.R.), Government of India for a Junior Research Fellowship.

References

- [1] A.L.Barabasi and H.E.Stanley *Fractal Concepts in Crystal Growth* (Cambridge University Press, 1995).
- [2] S.F.Edwards and D.R.Wilkinson Proc.R.Soc. London, Ser.A 381 17 (1982).
- [3] A.L.C.Ferreira, S.K.Mendiratta and E.S.Lage J.Phys.A:Math. Gen. 22 L431 (1989).
- [4] D.B.Abraham and P.J.Upton Phys. Rev. B 39 736 (1989).
- [5] M. Barma, *Non Linear Phenomenona in Materials Science III Solid State Phenomena Vol. 42-43*, G. Ananthakrishna, L.P. Kubin and G. Martin, Eds. (SciTech Publications Ltd. Switzerland, 1995)
- [6] A.L.C.Ferreira and S.K.Mendiratta J.Phys. A:Math.Gen. 24 4397 (1991).
- [7] Mustansir Barma J.Phys. A:Math.Gen. 25 L693 (1992).
- [8] S.N.Majumdar and M.Barma Phys. Rev. B 44 491 (1991).
- [9] S.N.Majumdar and M.Barma Physica 177A 366 (1991).
- [10] M.Kardar, G.Parisi, and Y.C.Zhang Phys.Rev.Lett. 56 889 (1986).
- [11] R. W. Cahn and P. Haasen *Physical Metallurgy* (North-Holland, Amsterdam, 1996).
- [12] M. Rao and S. Sengupta Phys. Rev. Lett. 78 2168 (1997); M. Rao and S. Sengupta, Curr. Sc. 77 382 (1999).
- [13] P. M. Chaikin and T. C. Lubensky *Principles of condensed matter physics*, (Cambridge University Press, Cambridge, 1995).
- [14] T.M.Ligget Interacting Particle Systems (New York: Springer)(1985).
- [15] N.Rajewsky et al arXiv:cond-mat/9710316v2 (1997).